



A greedy algorithm for wavelet-based time domain response spectrum matching

Jinsuo Nie^{*}, Vladimir Graizer, Dogan Seber

U.S. Nuclear Regulatory Commission, 11555 Rockville Pike, Rockville, MD 20852, USA



ARTICLE INFO

Keywords:
 Greedy algorithm
 Wavelet
 Time domain
 Response spectrum matching
 Zero-period acceleration
 Seismic time history analysis

ABSTRACT

U.S. Nuclear Regulatory Commission NUREG-0800, "Standard Review Plan," Section 3.7.1, "Seismic Design Parameters," Revision 4, describes acceptance criteria for seismic design time histories, including response spectrum matching and checking power spectral density functions. This paper is a focused introduction of a new algorithm developed for response spectrum matching, named as the Greedy Wavelet Method (GWM), which shows substantial advances in convergence characteristics over the RspMatch09 program. RspMatch09 is widely used by the nuclear industry and represents the results of multiple iterations of enhancement by international researchers since the basic method was first introduced in 1978. GWM modifies a seed acceleration time history by adding just one wavelet in each iteration, in contrast to RspMatch09 that adds a set of weighted wavelets, with the weights determined by solving an optimization problem in each iteration. GWM includes procedures to address two specific issues leading to convergence difficulties in response spectrum matching: The shape of the wavelets can be numerically distorted at high frequencies and the wavelet lead time previously recommended is not sufficiently long. These newly developed procedures made GWM unconditionally stable. For the benchmark problem, GWM was demonstrated to save 99.5% of the wavelets required by RspMatch09. We also implemented in GWM several advanced, interactive tools to perform baseline corrections and other related tasks. Examples provided in this paper are for demonstration purposes only.

1. Introduction

Seismic time histories are widely used in seismic analysis, qualification, and evaluation of critical structures. The time histories to be used in these analyses can be developed using various procedures to modify seed records. The procedures may include spectral amplitude scaling at the structure's fundamental frequency, spectral matching in a select frequency range, or scaling to the expected peak ground acceleration (PGA). The choice of the acceleration time history modification methods is often dictated by industry standards and codes. Some standards allow the use of only one time history while others require three to seven (NEHRP, 2011). When selecting seed records it is recommended to consider the design earthquake magnitude, fault mechanism, epicentral distance, and local site effects (e.g., ASCE/SEI 7-05, 2006; ASCE 41-06, 2007; ASCE/SEI 4-16, 2017; ASCE/SEI 43-19, 2019; etc.). Other considerations for developing acceleration time histories include the selection of time increment, strong motion duration, the ratios V/A and AD/V² (A, V, D are peak ground acceleration, peak ground velocity, and peak ground displacement, respectively). In particular, for response

spectrum (RS) matched acceleration time histories, it is also important to check the sufficiency of their power spectral density (PSD) functions because power-deficient design time histories can lead to significant underprediction of in-structure response spectra and other frequency-sensitive structural responses. The necessity of PSD checks applies to both a single set and multiple sets of acceleration time histories (U.S. Nuclear Regulatory Commission (USNRC), 1989; Nie et al., 2019; Nie, 2020; Nie et al., 2020; 2023). NUREG-0800, Standard Review Plan, U.S. Nuclear Regulatory Commission, Revision 4 of Section 3.7.1. (USNRC, 2014b), "Seismic Design Parameters," describes acceptance criteria for seismic design time histories that include both RS matching criteria and PSD checks against target PSD functions compatible with the design response spectra (DRS).

Provided that all these aspects are adequately addressed at various stages in the development of acceleration time histories, this paper is devoted to a focused introduction of a new method for RS matching to ensure the acceleration time histories meet the RS convergence requirements.

For critical structures such as nuclear power plants (USNRC, 2014a,

* Corresponding author.

E-mail address: Jinsuo.nie@nrc.gov (J. Nie).

2014b), the most common approach to developing acceleration time histories is to modify recorded earthquake accelerations using one of the many RS matching algorithms (e.g., Lilhanand and Tseng, 1988; Abrahamson, 1992; Hancock et al., 2006; Al Atik and Abrahamson, 2010; Shahbazian and Pezeshk, 2010; Huang et al., 1998; Li et al. 2016, 2017; and Ni et al., 2013). The RS-matching algorithms can be generally categorized as frequency domain methods or time domain methods. The frequency domain methods usually preserve the Fourier phase spectra of the seed records well, while the time domain methods usually preserve well the basic nonstationary features of the seed records in the time domain. It is well recognized that the time domain methods have better convergence properties than the frequency methods although the time domain methods are usually more complicated to implement. In general, RS matching should start with a seed record that has a spectral shape similar to the design response spectrum, because such a record usually requires less modification so its original characteristics can be better preserved (NEHRP, 2011; Vemuri and Kolluru, 2020).

The algorithm developed in this paper follows the time domain wavelet-based methods proposed by Kaul (1978) and Lilhanand and Tseng (1988) and subsequently enhanced by Abrahamson (1992), Hancock et al. (2006), and Al Atik and Abrahamson (2010). In these methods, one needs to repeatedly add wavelets to the ground motion records until the RS convergence criteria are met. Kaul (1978) was the first to propose an optimization procedure to perform time domain spectral matching and Lilhanand and Tseng (1988) extended that method to simultaneously match response spectra at multiple damping values. Abrahamson (1992) used a tapered cosine wavelet to replace the original reverse acceleration impulse response wavelet in order to preserve the time domain nonstationary characteristics of the seed records and ensure stability and efficiency of the algorithm. Hancock et al. (2006) further proposed a baseline-corrected tapered cosine wavelet that has zero initial and final displacement so that the resultant acceleration time history does not require baseline correction. This method however is considered to be less efficient due to its use of numerical integration and it sometimes has difficulty in achieving convergence. In the most recent update of this method, Al Atik and Abrahamson (2010) proposed an improved tapered cosine wavelet that employs a bell shape as the taper function to replace the exponential taper function proposed by Abrahamson (1992). The improved tapered cosine wavelet allows analytical solution and integrates to zero velocity and displacement, so baseline correction of the converged time history is not necessary. The program developed by Al Atik and Abrahamson (2010) is known as RspMatch09.

Although these wavelet-based time domain RS-matching methods differ in their wavelet functions, they use the same optimization scheme to obtain the weights for the wavelets in every iteration. The solution of the optimization problem in each iteration of the algorithm requires creating and inverting a square matrix that has a size equal to the number of spectral points used for RS matching. That square matrix, the so-called C matrix, consists of the oscillator maximum responses subjected to the wavelets at all frequencies considered in RS matching.

To address a research need to estimate the uncertainties in in-structure response spectra due to uncertainties in RS-matched input acceleration time histories, we needed to automatically generate thousands of RS-matched acceleration time histories (Nie et al., 2023). We initially considered using the RspMatch09 program to take advantage of its speed and accessibility. However, the high number of RS-matched time histories required a higher level of automation. To accomplish this, we chose to use the Python programming language to develop a new program so that processing thousands of seed records would be efficient. We initially considered to develop a Python implementation of the algorithm described by Al Atik and Abrahamson (2010), but our research needs eventually led to our development of a new greedy algorithm that is more convenient to implement and shows substantial advances in convergence performance for RS matching. We call this method and its associated set of auxiliary tools as the Greedy Wavelet

Method (GWM) for easy reference in this paper. GWM is fundamentally different from RspMatch09 and its predecessors, although it utilizes the same improved tapered cosine wavelet introduced by Al Atik and Abrahamson (2010). GWM adds just one wavelet to the seed record in each iteration, and does not need to solve the optimization problem.

In this paper, we introduce the basic procedure of GWM and document specific procedures to make GWM unconditionally stable. These procedures were introduced to address, among other things, two specific issues we found that lead to convergence difficulties in response spectrum matching: The shape of the wavelets can be numerically distorted at high frequencies and the wavelet lead time previously recommended is not sufficiently long. As to be demonstrated in the rest of this paper, GWM requires a significantly smaller number of wavelets than RspMatch09, indicating much smaller modifications to the seed records. Therefore, GWM makes possible a well separated treatment of power assurance and RS matching. The users of GWM can first introduce sufficient power to seed time histories based on the target PSD functions, and then apply GWM to achieve RS convergence criteria without much concern of making the final time histories deficient of power.

The resultant time histories using GWM require baseline corrections, hence we implemented methods to make the baseline corrections easy to apply. The current algorithm uses only one DRS, but it is possible to expand it to multiple DRS. We demonstrate the effectiveness and efficiency of the algorithm through examples. The examples provided in this paper use 5%-damped absolute acceleration response spectra. However, the algorithm does not mandate what type of RS is used as long as the DRS and the calculated RS are of the same type.

2. Basic procedure for GWM

In our description of GWM, we use symbols and terminologies similar to those used by Al Atik and Abrahamson (2010). We define $a_0(t)$ as the seed acceleration record. To modify $a_0(t)$, GWM repeatedly adds one wavelet at a time until the computed response spectrum $R(f)$ of the resultant acceleration time history $a(t)$ matches the design response spectrum $Q(f)$ across the entire frequency range of interest within certain prescribed convergence criteria. The terms t and f refer to time and frequency, respectively.

For convergence check, the response spectrum $R(f)$ of the modified acceleration time history is numerically compared to the design response spectrum $Q(f)$ at N prescribed frequencies. If the spectral values at the i^{th} frequency (f_i) are R_i and Q_i , the spectral difference at this frequency is defined as:

$$\Delta R_i = (Q_i - R_i)P_i \quad (1)$$

Where P_i indicates the polarity of the peak response of the oscillator at frequency f_i . If the maximum response of the oscillator subjected to $a(t)$ is positive, P_i is equal to 1; otherwise, P_i is equal to -1. When P_i equals 1, a positive ΔR_i indicates that the computed response spectral value is below the design value, and the wavelet to be added to $a(t)$ needs to increase R_i . When P_i equals -1, a positive ΔR_i indicates that the computed response spectral value is above the design value, and the wavelet added to $a(t)$ needs to reduce R_i . Therefore, the algorithm to compute the response spectrum of $a(t)$ or a wavelet needs to have a capability to return the spectral value, and the polarity and the time when the spectral value occurs in the response time history.

Given Equation (1), RspMatch09 and its predecessors solve a series of optimization problems until convergence is achieved. At each iteration, N wavelets are added with scaling factors determined by solving an optimization problem (setting up and inverting a square matrix), at the N prescribed frequencies for RS calculation and comparison. In contrast, GWM first determines the maximum spectral difference ΔR_{\max} of the current iteration by:

$$i_{max} = \operatorname{argmax}_{1 \leq i \leq N} |\Delta R_i| \quad (2)$$

$$\Delta R_{max} = \Delta R_{i_{max}}$$

Then, a wavelet of frequency $f_{i_{max}}$ with a maximum response of ΔR_{max} and a proper polarity according to $P_{i_{max}}$ is added to $a(t)$. GWM then repeats itself in the next iteration, starting with calculating the response spectrum of the updated $a(t)$ and using Equation (1) to get the series of ΔR_i . This process continues until convergence is reached or a prescribed number of iterations M is reached.

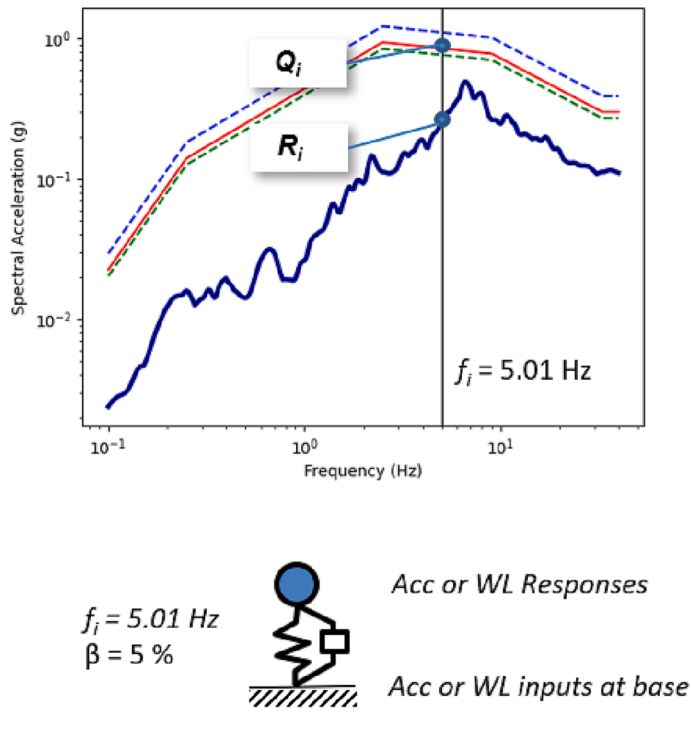
GWM uses the same wavelet (improved tapered cosine wavelet) as described by Equation (16) in Al Atik and Abrahamson (2010):

$$w_i(t) = \cos(\omega'_i(t - t_i + \Delta t_i)) \exp\left(-\left(\frac{t - t_i + \Delta t_i}{\gamma_i}\right)^2\right) \quad (3)$$

Where the damped frequency $\omega'_i = \omega_i \sqrt{1 - \beta^2}$, for frequency ω_i and damping β (5% in this paper); t_i is the time when the response of the oscillator of frequency ω_i achieves its maximum; Δt_i is the wavelet lead time, the difference between the peak response time t_i and the center of the wavelet (the “reference origin” as in Al Atik and Abrahamson (2010)); and γ_i is a frequency dependent coefficient to control the width of the wavelet.

The wavelet lead time Δt_i is defined as:

$$\Delta t_i = \frac{\tan^{-1}\left(\frac{\sqrt{1-\beta^2}}{\beta}\right)}{\omega'_i} \quad (4)$$



Anatomy of Wavelet-Based Time Domain RS-Matching

The purpose of Δt_i is to place the center of the wavelet before t_i so that the wavelet and $a(t)$ cause the oscillator of frequency ω_i to reach its peak responses at the same time t_i . This is to ensure that the wavelet mainly adjusts the maximum response of the oscillator, but causes less impact on the other parts of the oscillator response.

The parameter γ_i controls the width of the wavelet and ensures a smooth taper (the bell shape function in Equation (3)) that includes several cycles of the cosine function and therefore aims at resulting in zero residual velocity and displacement at all frequencies. For any frequency f , the continuous form of γ_i is defined by the following empirical equation as in Al Atik and Abrahamson (2010):

$$\gamma(f) = 1.178 f^{-0.93} \quad (5)$$

This empirical equation is similar to the reciprocal of f , but several trials appeared to indicate the above equation performed better in terms of convergence rate.

At the m^{th} iteration, the acceleration time history is updated by adding a wavelet of frequency $f_{i_{max}}$ multiplied by the following factor:

$$b_{i_{max}} = \Gamma \bullet \Delta R_{max} \bullet \frac{P^{w_i}}{R^{w_i}} \quad (6)$$

Where Γ is a relaxation parameter between 0 and 1, and P^{w_i} and R^{w_i} are the polarity and the absolute maximum value of the response history of an oscillator of frequency $f_{i_{max}}$, with damping β (5%), and subjected to the wavelet w_i in Equation (3). The relaxation parameter Γ has been set to 1 in GWM, and its convergence rate has been found to be quite acceptable. The effect of Γ on further improving convergence rate remains as a future exploration.

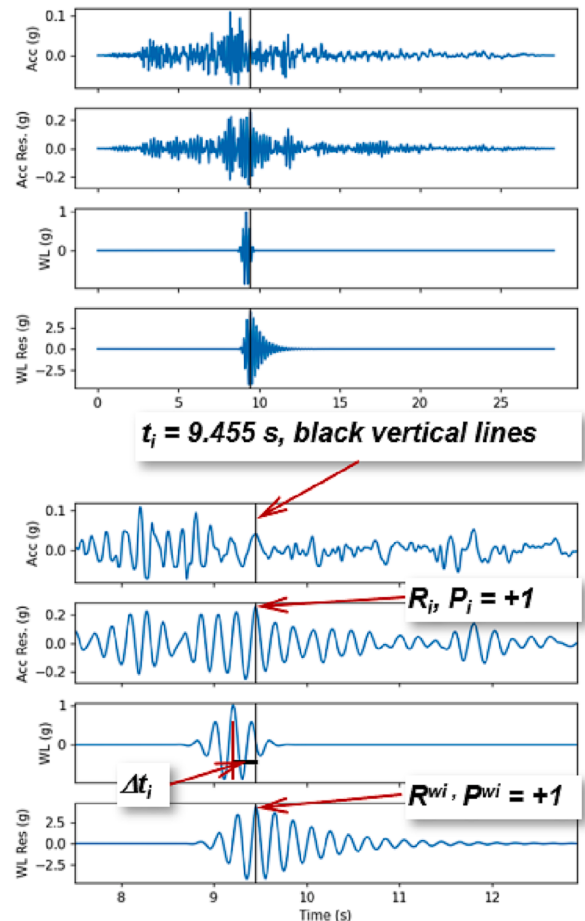


Fig. 1. Illustration of wavelet-based time domain RS-matching scheme with symbols defined in Section 2. The wavelet at frequency f_i is placed at $t_i - \Delta t_i$ such that it causes the peak oscillator response to occur at the same time t_i as the acceleration time history does. The time history plots at the top right corner show the entire time duration, while those at the bottom right corner show zoomed-in views to show the details around the peak response time t_i .

The procedure described above is a complete set of steps for GWM. The last step, in which a wavelet multiplied by $b_{i_{max}}$ is added to $a(t)$, is comparable to Equation (11) in [Al Atik and Abrahamson \(2010\)](#), with which RspMatch09 adds a weighted sum of all N wavelets to $a(t)$.

Although their basic procedures are fundamentally different, both RspMatch09 and GWM share the same logic in adding a wavelet w_i to the acceleration time history $a(t)$. Both methods aim at ensuring w_i and $a(t)$ would cause the oscillator at frequency f_i to achieve its maximum responses at the same time, but potentially with different polarities. [Fig. 1](#) shows an illustration of adding a wavelet to an acceleration time history, using the symbols defined in this section. The wavelet is placed with a time difference Δt_i before t_i when the peak response of the oscillator subjected to the acceleration time history occurs, such that the oscillator peak response due to the wavelet also occurs at t_i .

3. GWM implementation details

This section provides some essential implementation details for

GWM, such as improvement of robustness of the algorithm, faster convergence, initial scaling, etc. These special aspects are discussed in this section, so that the basic procedure described above remains pure and simple.

3.1. Enhancement to the wavelet lead time Δt_i and polarity

The basic procedure introduced above had many successes in real applications. However, in some cases the procedure resulted in divergence at higher frequencies, as shown in [Fig. 2](#). These divergence issues at high frequencies can be attributed to multiple issues. However, most of these divergence issues can be resolved by performing RS matching in separate frequency ranges, for example, a high frequency range (10–100 Hz), then a mid-frequency range (1–10 Hz), and lastly a low frequency range (0.1–1 Hz). Our implementation of GWM has interactive capabilities through a graphical user interface (GUI) to facilitate RS matching within specific frequency bands. It should be noted that there is a similar recommendation in RspMatch09 for passes with different

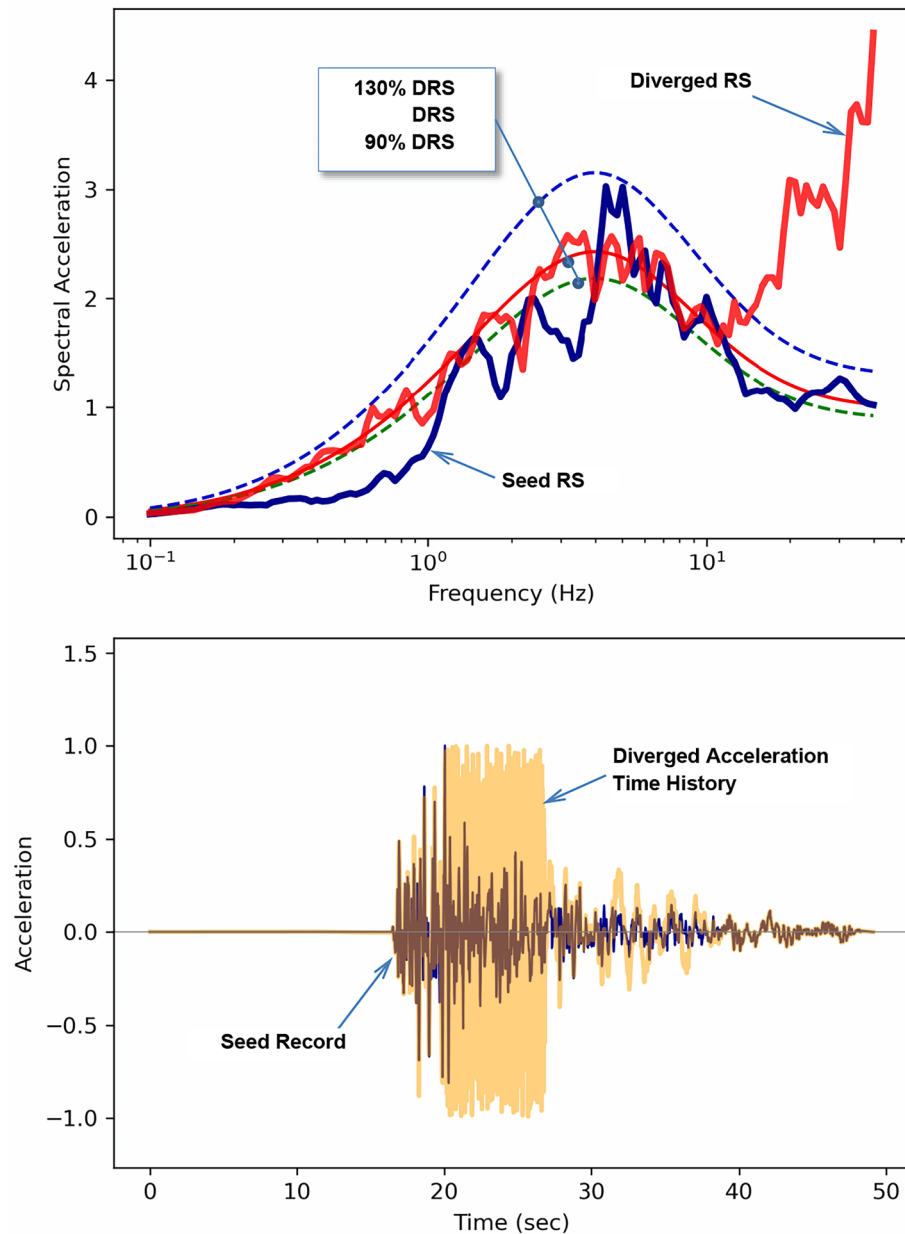


Fig. 2. Example of the basic procedure that diverges at high frequencies.

frequency bands, and the example coming with the RspMatch09 program has four progressive frequency bands 1–35 Hz, 0.5–35 Hz, 0.3–35 Hz, and 0.1–35 Hz in four runs of the RspMatch09 program. The GWM GUI allows frequency bands to be arbitrarily selected.

In order to make GWM more useful for our research need that involved in performing RS matching on thousands of seed acceleration records, we explored the root cause for such divergence cases so that GWM can be used in an automated fashion (Nie et al. 2023). We found that in general the wavelet lead time Δt_i as expressed in Equation (4) is not long enough to ensure that the maximum oscillator response of the wavelet occurs at the same time of the acceleration time history, as shown by Fig. 3.

A possible reason Equation (4) does not provide an adequately long wavelet lead time is that the new bell shape taper function is a lot wider at the center than the exponential taper function, for which Equation (4) was introduced. For the improved wavelet function, Al Atik and Abramson (2010) did not propose a new Δt . The figure below shows the difference between the taper functions (Fig. 4).

We also found that the wavelet defined by Equation (3) does not have a uniformly smooth waveform across the frequency range of interest due to sampling rate limitations. This can compound the effect of the wavelet lead time Δt_i being too short. We noted that as the frequency increases, the width of the wavelet gets narrower in the time domain and at higher frequencies fewer points are sampled in defining the wavelets because the time increment is kept constant. Fig. 5 shows wavelets of frequencies 0.5 Hz, 5 Hz, 19.443 Hz, and 34 Hz, showing that the smoothness and the shape of the wavelets are adequately represented at lower frequencies, but they gradually become distorted at higher frequencies.

Reducing the time step increments, effectively increasing the sampling rate, can improve the numerical representation of the high frequency wavelets and may be used to enhance the overall robustness of the GWM. However, for engineering purposes, the time step is also a result of practical considerations for seismic analysis, and may not need to be as high as those required to achieve a smooth representation of the high frequency wavelets. If the sampling rate is temporarily increased for the purpose of better wavelet representation, and the resultant acceleration time history is resampled back to the original sampling rate for seismic analysis, the final acceleration time history may not meet the RS convergence criteria. Additionally, the only shared goal of the many methods for RS-matching in the literature is to meet the RS convergence criteria and because these methods rely on vastly different approaches, the net effective modification achieved in the final acceleration time histories relative to their seed records may not resemble any combinations of nicely represented wavelets. More specifically, wavelet-based

methods for RS-matching may employ different types of wavelets and the converged acceleration time histories may not be sensitive to the smoothness of the wavelets. Wavelets in these methods are used to introduce perturbations to the acceleration time histories, and there are no specific physical requirements about their smoothness. The method described in the following is what has been implemented in the current GWM to explicitly align the numerical response of the oscillator subjected to a wavelet to the oscillator response due to the acceleration time history.

The effects of the numerically distorted high frequency wavelets may include introduction of drift in velocity and displacement time histories as well as a shift in the oscillator's peak response time and its polarity. To address these issues associated with numerically distorted wavelets and with Equation (4), GWM uses a procedure to calculate the response spectrum of a wavelet to explicitly return the location of the oscillator peak response. This capability is also required for calculating the response spectra of an acceleration time history for all wavelet-based RS matching methods introduced at the beginning of this paper. If the location of the oscillator peak response subjected to a wavelet w_i is $t_i^{w_i}$, the actual wavelet lead time Δt_i is simply defined as:

$$\Delta t_i = t_i^{w_i} - t_i \quad (7)$$

Which is then used to shift the wavelet location such that the peak oscillator responses from the wavelet w_i and from the acceleration time history $a(t)$ are aligned.

For wavelets defined by Equation (3), the polarity of the oscillator response is equal to 1 in theory and in most numerical cases. Therefore, the wavelet polarity p in Equation (6) is usually not needed. In fact, it does not even exist in the derivations for RspMatch09 and its predecessors because it is theoretically equal to 1. However, we found that some numerically distorted wavelets may actually make $P^{w_i} = -1$, consequently requiring a flip of the wavelet by explicitly considering the wavelet polarity P^{w_i} in Equation (6). Returning polarity from response spectrum calculation is another capability required by all the wavelet-based RS matching methods described in this paper. Therefore, the same algorithm to calculate the RS of the acceleration time history is reused to calculate the three quantities related to the maximum oscillator response due to the wavelet w_i , i.e., the absolute maximum value R^{w_i} , the polarity P^{w_i} , and the location $t_i^{w_i}$. In addition, the RS calculation for the wavelet w_i only needs to consider one frequency $f_{i,\max}$ in each iteration. Direct application of R^{w_i} , P^{w_i} , and $t_i^{w_i}$ allows GWM to be easily expanded to consider many other types of wavelets; for example, some limited applications of wavelets with the exponential taper function show better convergence rate than the bell shape taper function.

It should be noted that the issues identified in this section may not affect the convergence of RspMatch09, because it uses the optimization process to determine the best weights for the wavelets.

3.2. Zero Pre-Padding and maintaining the duration of the seed acceleration time history

The RspMatch09 algorithm requires dynamically zero padding the time history at the beginning of the acceleration time history. When t_i is small, Δt_i may require a wavelet w_i to start before the start of the acceleration time history. Zero pre-padding also intends to ensure the wavelets, especially low frequency wavelets, would not cause drift in velocity and displacement. RspMatch09 provides an empirical equation for the minimum t_i values that are required to prevent drift for different frequencies. The minimum t_i value is larger when frequency is lower; therefore, the effect of the minimum t_i mostly affects low frequency wavelets in practice. The minimum t_i is defined as (Al Atik and Abramson, 2010):

$$t_i^{\min} = 3.9223 \times f_i^{-0.845} \quad (8)$$

When t_i is lower than t_i^{\min} , the acceleration time history $a(t)$ is zero-

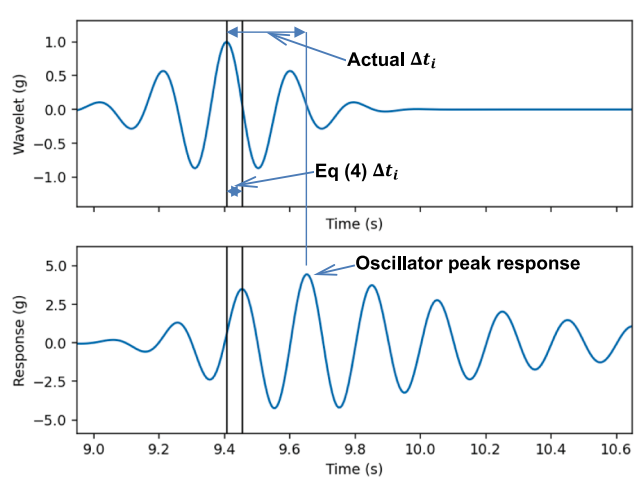


Fig. 3. Illustration of the wavelet lead time Δt_i by Equation (4) and the actual required lead time using a 5 Hz wavelet.

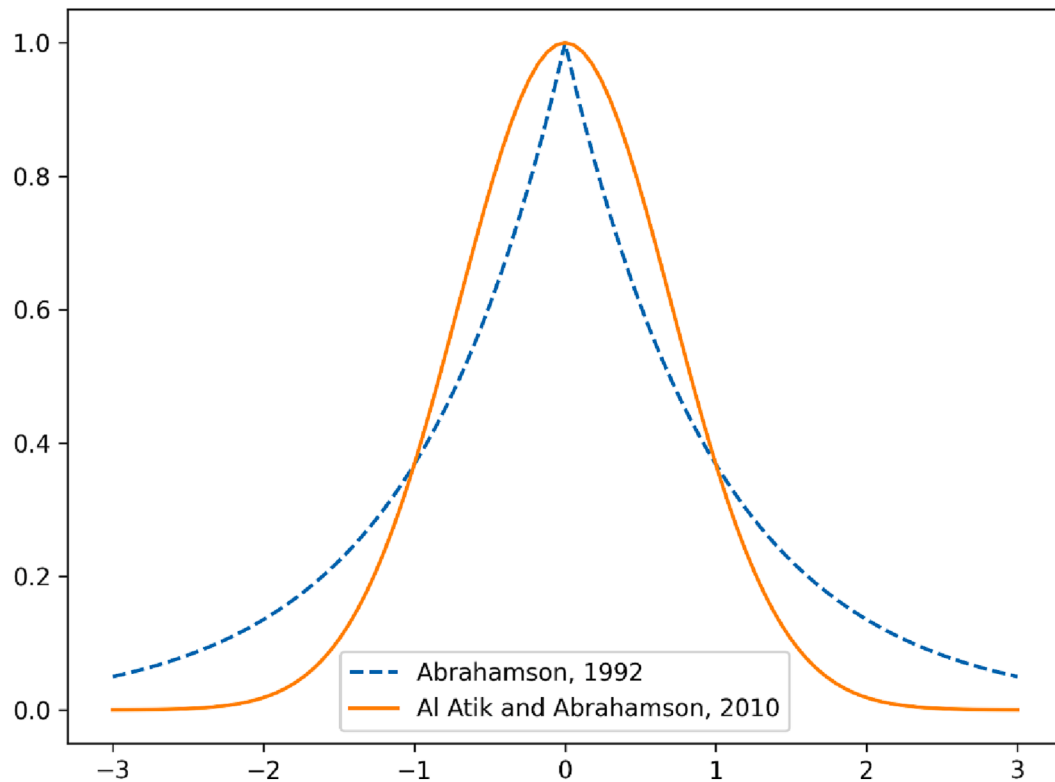


Fig. 4. Difference between the exponential taper function proposed by Abrahamson (1992) and the bell shape taper function proposed by Al Atik and Abrahamson (2010).

pre-padded such that t_i equals t_i^{\min} . GWM similarly pre-pads the seed acceleration record. While RspMatch09 dynamically performs such zero-padding during the RS matching process, GWM only performs this once on the seed acceleration record for all N frequencies considered for RS matching.

A zero pre-padded acceleration time history has a longer duration than its seed acceleration record. Although this may be acceptable in many cases, maintaining the same duration as the seed record is desirable in some other cases. For example, Fig. 6 shows an RS-matched acceleration time history that has a single wavelet added before the start of the seed acceleration record, making the resultant time history look unrealistic. Therefore, in such cases, the pre-padded portion of the resultant time history can be stripped to maintain the same duration as the seed record. However, the stripped acceleration time history usually does not have a zero starting acceleration, and its response spectrum may become unsatisfactory when compared to the DRS at the affected frequency. The former problem can be resolved by applying an envelope function to enforce the acceleration time history starts at zero, and the latter problem can be resolved by specifically adding a wavelet, usually at a low frequency, in the middle of the acceleration time history such that the spectral value of the resultant time history at this frequency occurs at a time away from the beginning of the acceleration time history. This will be discussed in more detail when the baseline correction is discussed later in this paper. Additionally, striping is one of the sources that cause drift in velocity and displacement of the final acceleration time histories.

3.3. Initial scaling

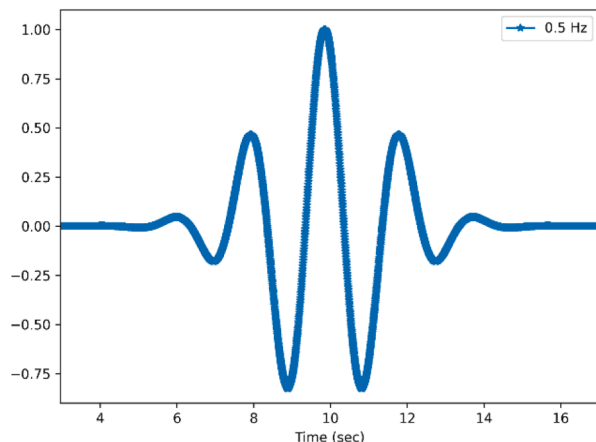
RspMatch09 recommends scaling the seed acceleration record before the first iteration to the peak ground acceleration in the first pass and no scaling in subsequent passes. RspMatch09 utilizes passes to perform RS-matching with different frequency ranges and other controlling parameters. Each pass typically includes a prescribed number of iterations,

and each iteration adds a weighted sum of wavelets at all oscillator frequencies. We also explored the benefits of initial scaling regarding convergence rate in GWM. Options included no scaling, scaling to PGA, scaling to peak spectral acceleration (PSA), and scaling using the geometric mean ratio of the DRS over the RS of the seed record for all frequencies in RS comparison. We found that scaling using the geometric mean ratio leads to the fastest convergence ratio, probably because the geometric mean ratio makes a linearly scaled seed record to have a computed RS closer to the DRS than other methods over the entire frequency range. Therefore, GWM defaults to this scaling method while other options are allowed as well.

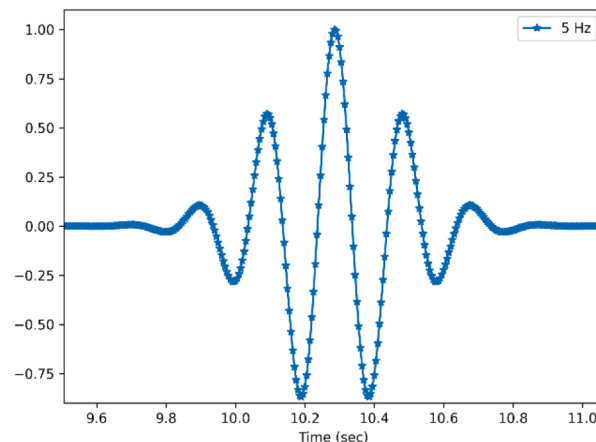
3.4. Zero period acceleration (ZPA) flipping

The ZPA, primarily used by engineers, is defined as the spectral acceleration computed using an extremely stiff oscillator (i.e., of zero period or infinite frequency), and is the spectral value at very high frequencies on a typical RS that levels off at higher frequencies. ZPA flipping is very important in achieving RS convergence for inadmissible DRS. For a response spectrum shape to be admissible, it has to decay sufficiently fast at the tail (toward higher frequencies) but cannot decay too fast in the same time as suggested by Pozzi and Der Kiureghian (2013). The same authors also noted that a given response spectrum may not be admissible for practical reasons. For example, some design spectra were developed by fitting simple functions to the response spectra of recorded ground motions and these functions, often piecewise linear functions, may not necessarily have admissible shapes at the tail. In terms of ZPA, time histories matched well in the periodic frequency range to the DRS are not able to produce a ZPA of the calculated RS close to the ZPA of inadmissible DRS. Therefore, ZPA flipping is often required for the calculated RS to have a ZPA similar to the ZPA on an inadmissible DRS.

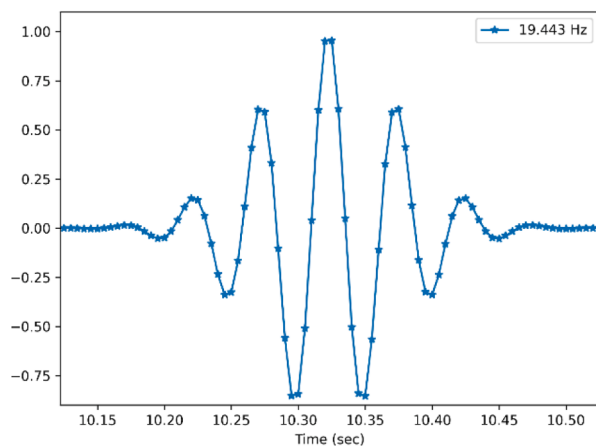
GWM achieves ZPA flipping by mirroring any acceleration points outside of the [-ZPA, ZPA] range around the lower or upper bound of



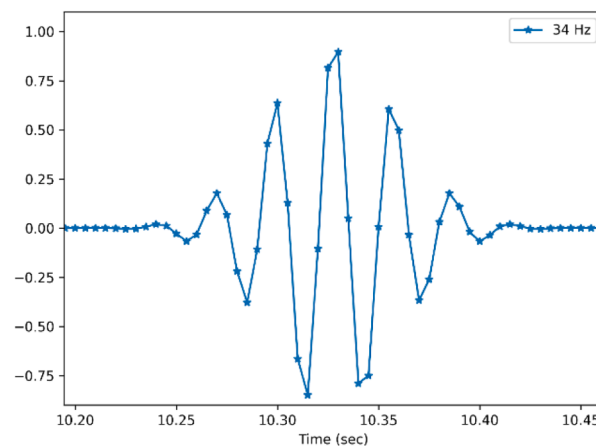
(a) A 0.5 Hz Wavelet



(b) A 5 Hz Wavelet



(c) A 19.443 Hz Wavelet



(d) A 34 Hz Wavelet

Fig. 5. The quality of wavelet representation degrades as frequency increases. All wavelets shown have the same time increment of 0.005 s, and plots (b), (c), and (d) are zoomed in to show shapes similar to plot (a).

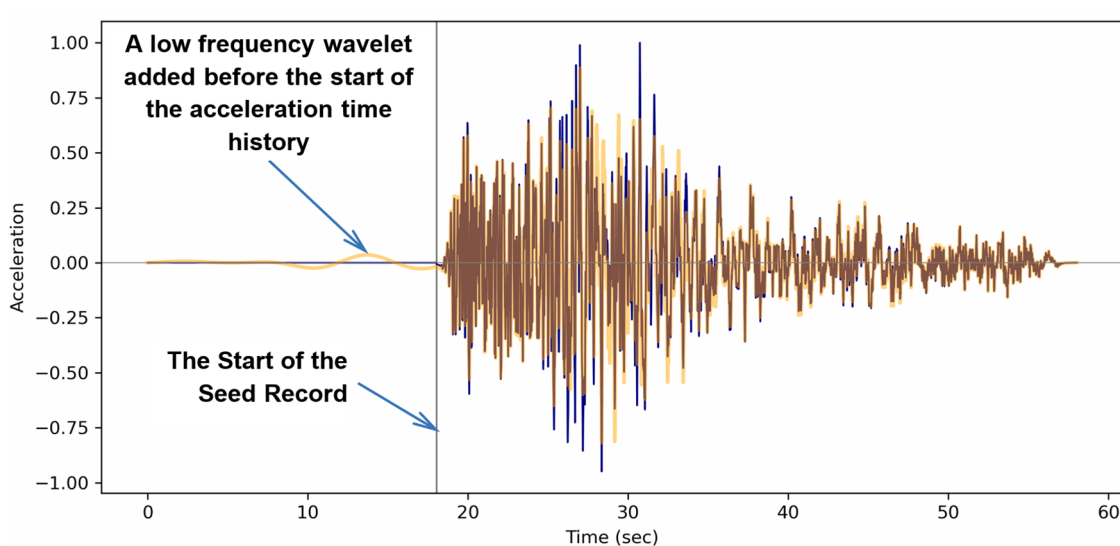


Fig. 6. An RS-matched time history that has a single low frequency wavelet added before the start of the seed acceleration record. The original seed record is shown in blue. The vertical line indicates the start of the seed acceleration record.

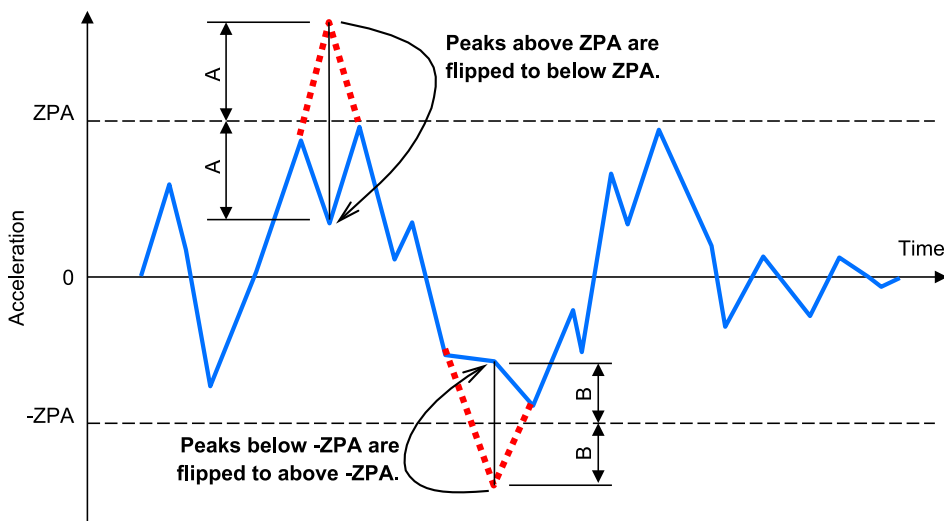


Fig. 7. Illustration of ZPA flipping. Red dashed tips are mirrored around ZPA or -ZPA because the points are outside of the [-ZPA, ZPA] range. The solid blue curve is after ZPA flipping. ZPA flipping helps maintain the ZPA of the acceleration time history close to the ZPA on the DRS.

this range. Fig. 7 illustrates how ZPA flipping is done. ZPA flipping can prevent GWM from constantly adding wavelets in the ZPA frequency range, attempting to bring the ZPA of the RS to match the ZPA of the DRS.

3.5. Convergence criteria specification

GWM has two ways to specify RS convergence criteria: symmetric match or for design. For symmetric match, the RS convergence criteria are applied equally above or below the DRS. For example, a 10% symmetric convergence criterion means the calculated RS is acceptable if it falls in the range of [90%, 110%] of the DRS. For design purposes, the RS convergence criteria are applied as is if RS is below the DRS; if RS is above DRS, the RS convergence criteria are tripled to favor more conservative calculated RS values. This is to simulate the popular criteria that the calculated RS is considered to be acceptable when it is within the [90%, 130%] range of the DRS.

It is noted that codes and standards may have additional criteria beyond the simple percentage criteria. For example, the current practice also requires a check on whether the calculated RS falls below the DRS for a large frequency window. The GWM basic procedure does not have such additional checks. However, a separate tool has been implemented in GWM for that check after the basic procedure indicates a converged RS has been achieved.

4. Benchmarking GWM against the RspMatch09 example

The RspMatch09 program is distributed with an example that can be used to benchmark GWM. This example provides a 5% damped DRS from 0.1 Hz to 100 Hz with 200 frequency points. Because RS matching is only conducted from 0.1 Hz to 35 Hz, the number of effective frequencies is $N = 169$. The seed acceleration record provided in the example has 5996 data points and a time interval of 0.005 s. The RS convergence criterion is 5% (symmetric). The example uses four passes that cover four frequency ranges, with varying lower frequency bound but constant higher frequency bound at 35 Hz. Therefore, each pass requires a different number of frequency points for RS calculation and comparison. The output file for the last pass indicates that RspMatch09 did not converge to the 5% criterion. We did not find a reason in the example files why the program stopped at 4 passes without additional passes until reaching the 5% convergence criterion, probably because the specified 5% convergence criterion was not intended to be fully met and the final check for convergence was based on a practical comparison

of the computed RS curve and DRS. Indeed, the maximum error after the last pass was reported in the output file to be 13.1%, and that is within a well acceptable level for design purposes. The figures provided by Al Atik and Abrahamson (2010) also show the good agreement between RS and DRS after 4 passes. We recently ran RspMatch09 on a cloud machine using this example and the execution of all 4 passes took about one minute. Four passes added a total of 9,070 wavelets.

We used this example to verify GWM. Fig. 8 shows the unscaled seed acceleration record, its RS, the DRS, as well as the 90%-DRS and 130%-DRS. The zero pre-padding and start of the seed record are also shown in the plot at the bottom of this figure. The RS is clearly much higher than the DRS across the entire frequency range from 0.1 Hz to 35 Hz. To achieve high convergence rate, we linearly scaled the seed record once with a factor as the geometric mean ratio of DRS over RS for all 169 frequencies, and the resultant seed RS is shown as the blue curve in the top plot of Fig. 9. The scaled seed RS is much closer to the DRS than the unscaled seed over all frequencies considered and it crosses the DRS curve between 1 Hz and 2 Hz.

Fig. 9 also shows the converged acceleration time history to the 5% RS convergence criterion, and GWM achieved convergence with merely 246 wavelets. The bottom plot of this figure shows that the converged acceleration time history conserves very well the nonstationary characteristics of the linearly scaled seed record and the differences between them are small.

GWM completed the RS matching for this example until converging to the 5% symmetric criterion in about 2 s on a laptop with 16 G memory and Intel 4 core i5-8350U CPU. The completion time varies somewhat because Python is an interpreted language, and reruns of the same matching problem often require less than 2 s. We were not able to run GWM and RspMatch09 on the same computer, but the cloud machine we used to run RspMatch09 was an Amazon AWS instance with faster CPU clock, more cores, and larger memory than the laptop we used for GWM. RspMatch09 is a Fortran program while GWM is a Python program. However, comparisons based on programming languages is more complicated because the algorithm to compute response spectra in GWM was a compiled Fortran extension module for Python that runs on 4 cores, while RspMatch09 is a single process program. Also, RspMatch09 appears to require more than 4 passes to achieve the convergence criterion of 5%. In summary, the GWM algorithm requires no optimization solution and uses a significantly smaller number of wavelets for RS convergence, indicating its computational advantages than RspMatch09. Therefore, the rest of the comparison will be based on the number of wavelets used to achieve RS convergence.

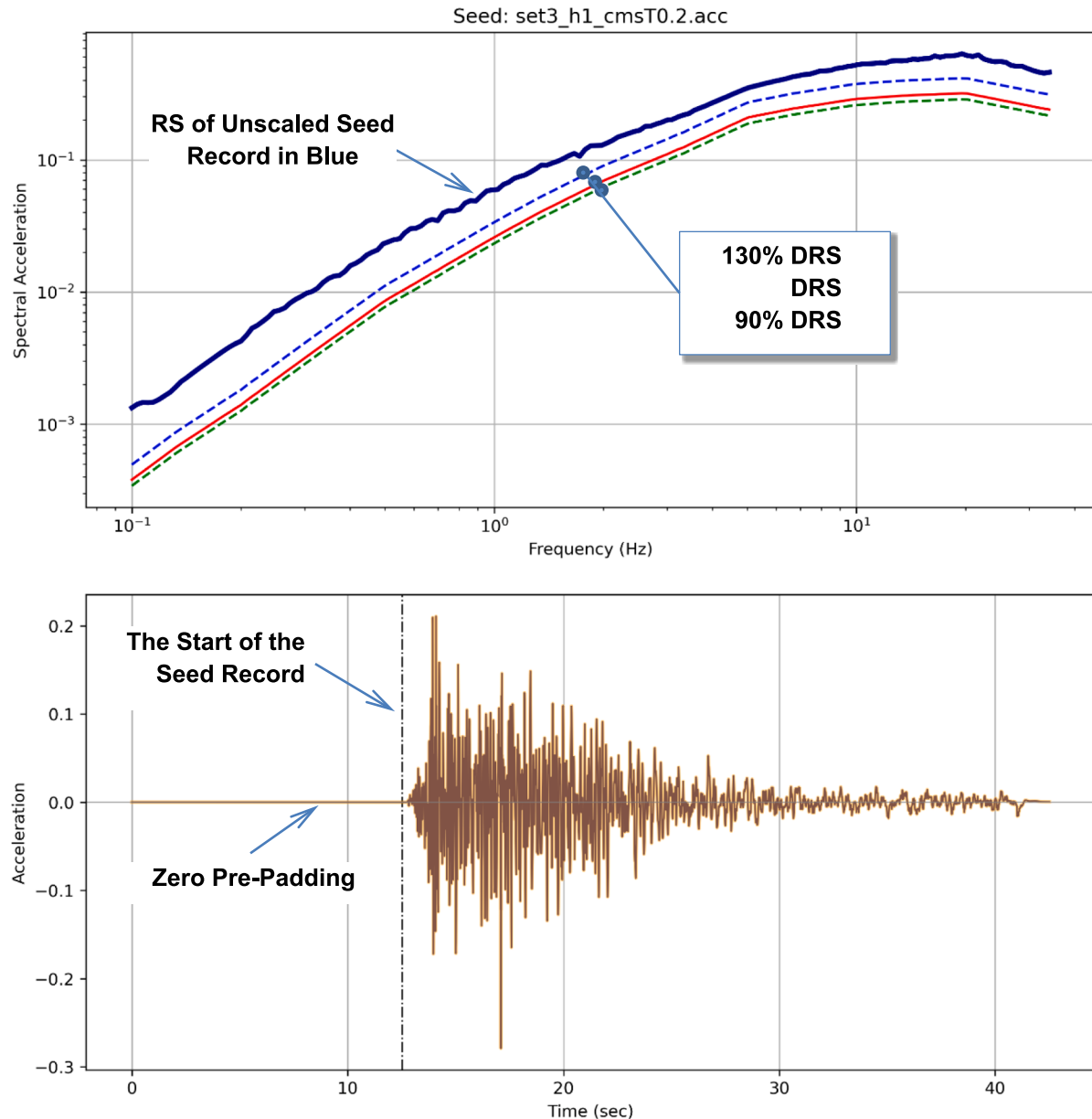


Fig. 8. The RspMatch09 example without scaling. The plot on the top shows the RS of the seed, the DRS and its [90%, 130%] bounds in dashed lines. The plot at the bottom shows the seed acceleration record with pre-padded zeros, where the dashed vertical line indicates the beginning of the seed record.

Fig. 10 shows the convergence history for GWM. It can be seen that GWM reduced the maximum error very quickly in the first few iterations, and the convergence rate gradually decreases as the RS gets closer to the DRS. For design purposes, the 5% convergence criterion may be considered very tight. When a 10% symmetric criterion was used (recall that the RspMatch09 example achieved a maximum error of 13.1% after 4 passes), GWM converged with just 46 wavelets and completed within 0.32 s. GWM used a substantially smaller number of wavelets than RspMatch09 (46 versus 9,070) based on the 10% RS convergence threshold. The number of wavelets used by GWM is even fewer than a third of the 169 wavelets that RspMatch09 uses in one iteration for the frequency range of 0.1 Hz to 35 Hz.

Fig. 11 shows the acceleration, velocity, and displacement time histories for the seed record, converged acceleration time history, and baseline (BL) corrected acceleration time history. GWM introduced minor drift to displacement and unnoticeable drift in velocity, because

of the numerically distorted high frequency wavelets and stripping the beginning portion of the converged acceleration time history before the start time of the seed record. ZPA flipping was not used for this example, so it was not a cause for the drift. The BL correction was achieved by using the displacement spline method, which is one of the several BL correction methods implemented in GWM. The interactive GUI provided in GWM allows BL correction achievable with a couple of mouse clicks and the entire calculation took a fraction of a second. The next section includes a dedicated introduction of the many methods implemented in GWM for BL correction.

Since GWM can be easily expanded to use different types of wavelets due to its direct use of the oscillator response of the wavelet and its convenient baseline correction methods, we had some preliminary results using the exponential taper function. Using the same gamma function as in Equation (5) to define the width of the wavelets, the number of wavelets was reduced to 209 and 43 to achieve the 5% and

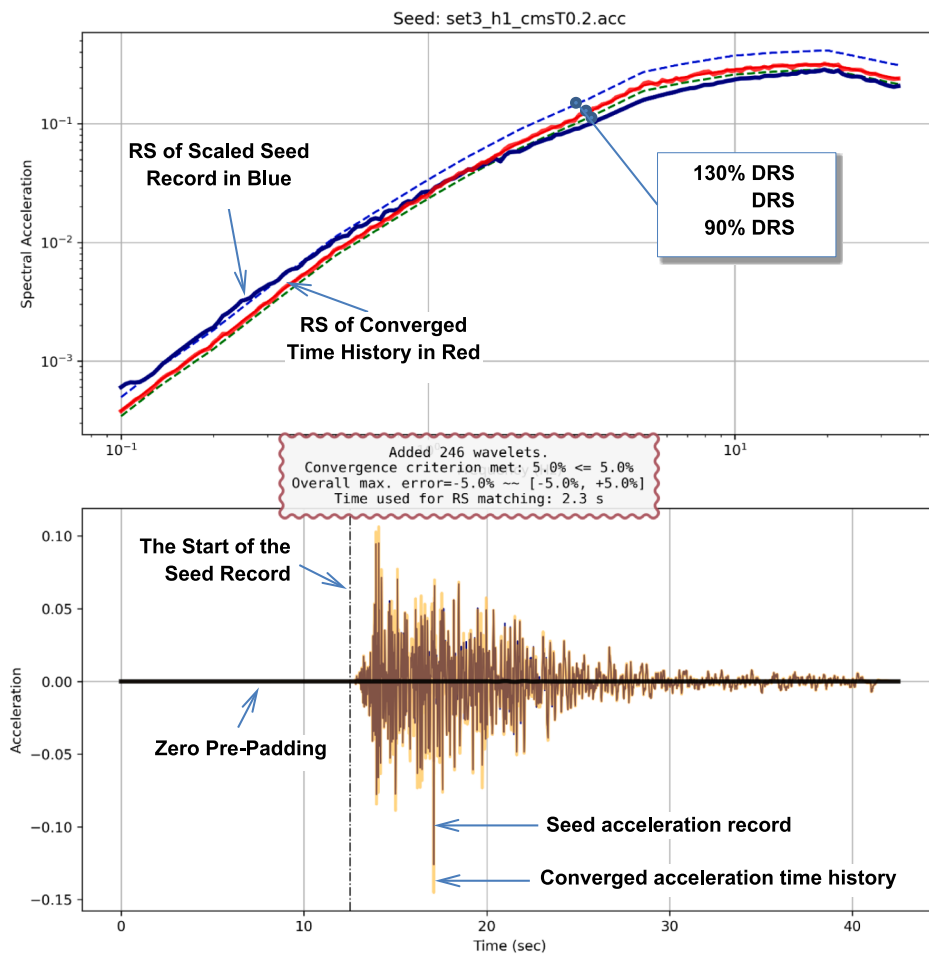


Fig. 9. The RspMatch09 example after GWM converged using a 5% symmetric convergence criterion. The box in the middle indicates a total of 246 wavelets were added to the seed record, and GWM took 2.3 s to complete on a laptop.

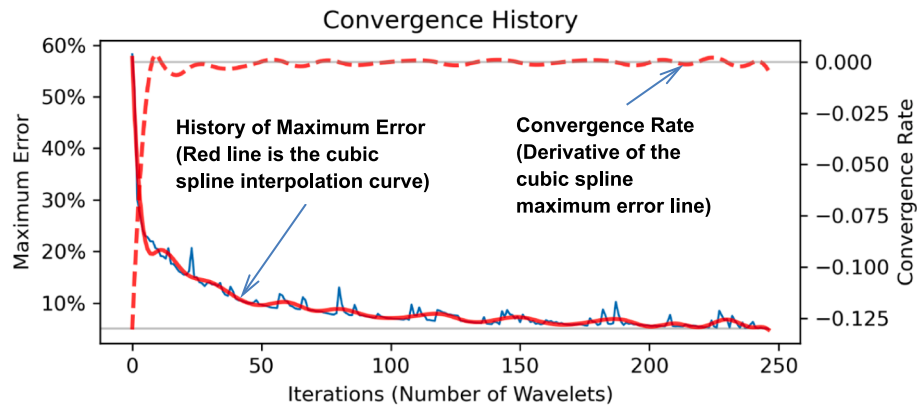


Fig. 10. GWM Convergence History for the RspMatch09 example. GWM reduces the maximum error in RS very quickly by adding only a few wavelets, after which GWM uses many more wavelet to fine tune the convergence.

10% symmetric convergence criteria, respectively. If the wavelet width is chosen as $1/(\beta \cdot \omega_i')$ (Hancock et al., 2006; Suarez and Montejo, 2005), the number of wavelets can be greatly reduced to 108 for the 5% symmetric convergence criterion, but remains the same as 43 for the 10% symmetric convergence criterion. The narrower-peaked wavelets perform better than the wider-peaked wavelets. These preliminary

results indicate a great potential for GWM to achieve the best RS convergence properties by identifying the optimal wavelet types and width parameters.

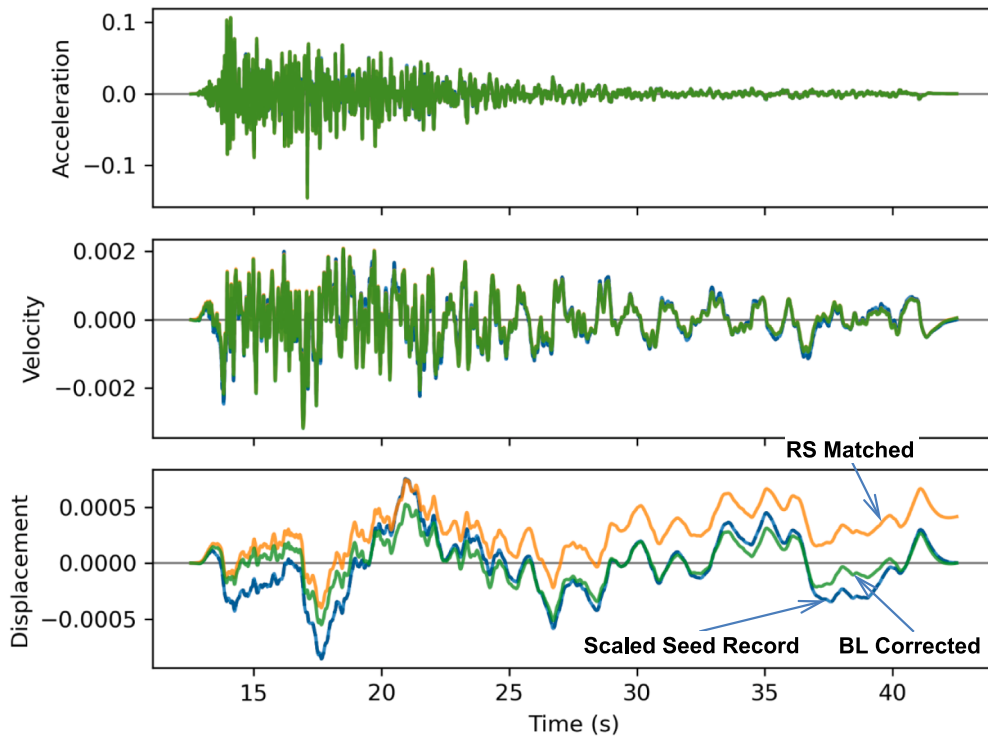


Fig. 11. Acceleration, Velocity, and Displacement History for the RspMatch09 example before and after RS matching. GWM introduced low level of displacement drift and some drift in velocity that is nearly unnoticeable. A baseline (BL) corrected displacement history is also shown and BL correction is consistently applied to velocity and acceleration but the effect is unnoticeable.

5. Baseline correction and other associated tools

GWM as a Python program can be extended very conveniently to add more functions. This section includes a focused introduction of some of the currently available functions, especially related to baseline correction. All baseline correction methods modify the acceleration time history directly, so the consistency between acceleration, velocity, and displacement is always enforced. Given the available tools for baseline correction, we do not see it is very necessary to require each wavelet not to introduce any residual velocity and displacement; therefore, many different types of wavelets can be explored in the future. Baseline correction can be performed once at the end of the process for acceleration time history development. For many engineering seismic analyses, the drifts in input motions do not affect the intended results because only structural deformations matter. However, there are many other types of seismic analyses requiring a removal of the unrealistic drifts, for example, to consider nonlinear behaviors, multiply supported systems subjected to different input motions, clearance between structures, etc.

GWM implemented several methods for baseline corrections, from simply removing the mean acceleration, to detrending a velocity time history, and to detrending displacement time history using polynomials up to 12th order, cubic splines, a Lagrange optimizer-based method (Borsoi and Ricard, 1985), and even an ongoing exploration using the Ensemble Empirical Mode Decomposition (Wu and Huang, 2008). These methods have various successful cases for different time histories, and we found the cubic spline method on the displacement time history was more robust than other methods in many cases. In addition, these methods can be applied consecutively to deal with some difficult cases.

Fig. 12 through 15 show the GUI interfaces to perform baseline correction based on detrending the velocity history using cubic splines, detrending the displacement time history using cubic splines, detrending the displacement time history based on a Lagrange optimizer, and detrending the displacement time history using polynomials,

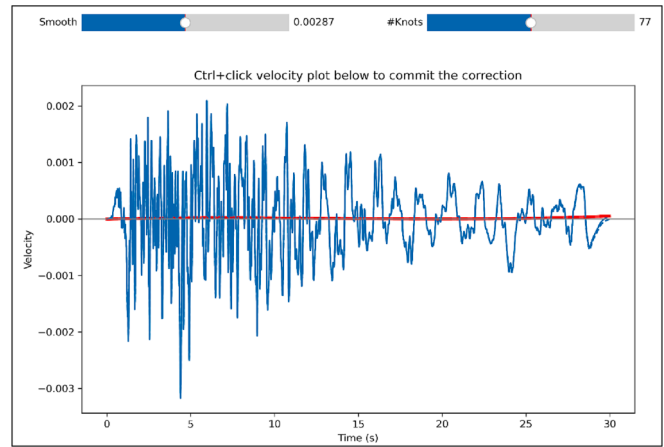


Fig. 12. Interface for detrending the velocity time history using cubic splines.

respectively. Although the default values for various parameters usually are satisfactory in these tools, they allow interactively changing the parameters to show the intended results. The common scheme for these tools is that the detrending functions need to be at least second-degree differentiable for detrending displacement and at least first degree differential for detrending velocity in order to make the modification in velocity or displacement be consistently transferred to the acceleration time history.

It should be noted that after baseline correction or stripping the zero pre-padded time period, the computed RS of some converged acceleration time histories would not compare well to the DRS, and that happens almost always in the very low frequency range. In such cases, additional matching using GWM would simply add very low frequency wavelets

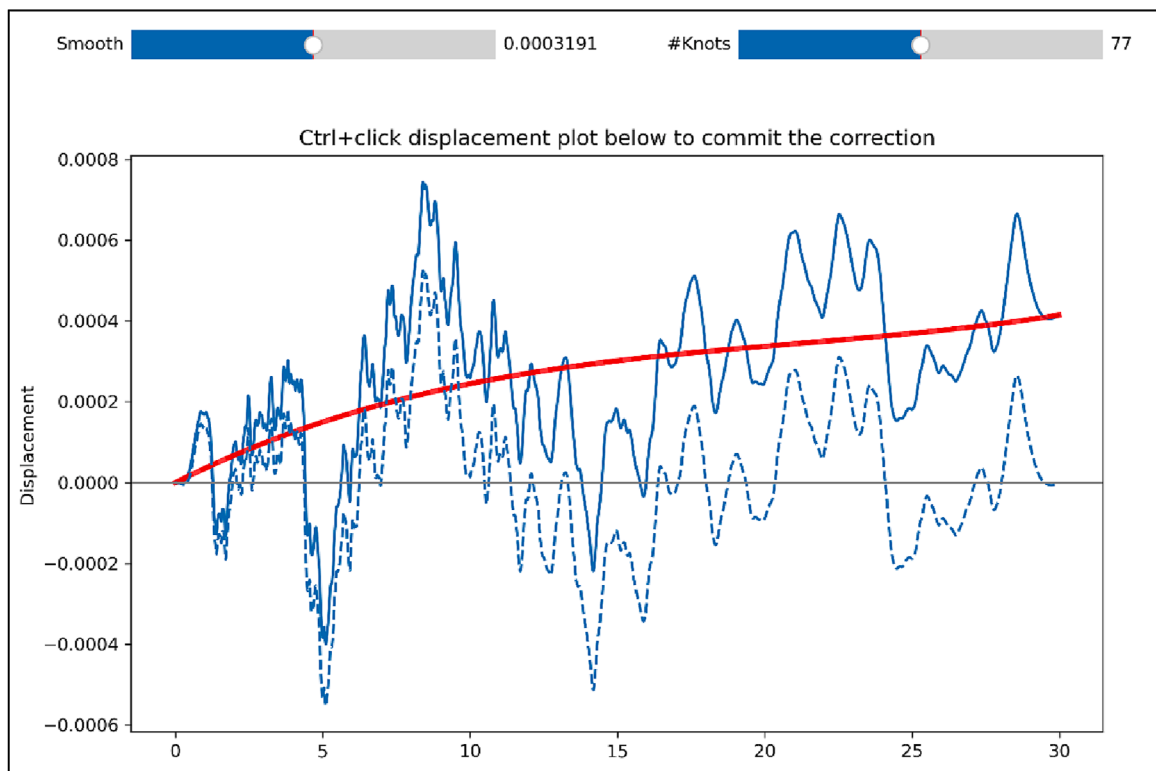


Fig. 13. Interface for detrending the displacement time history using cubic splines.

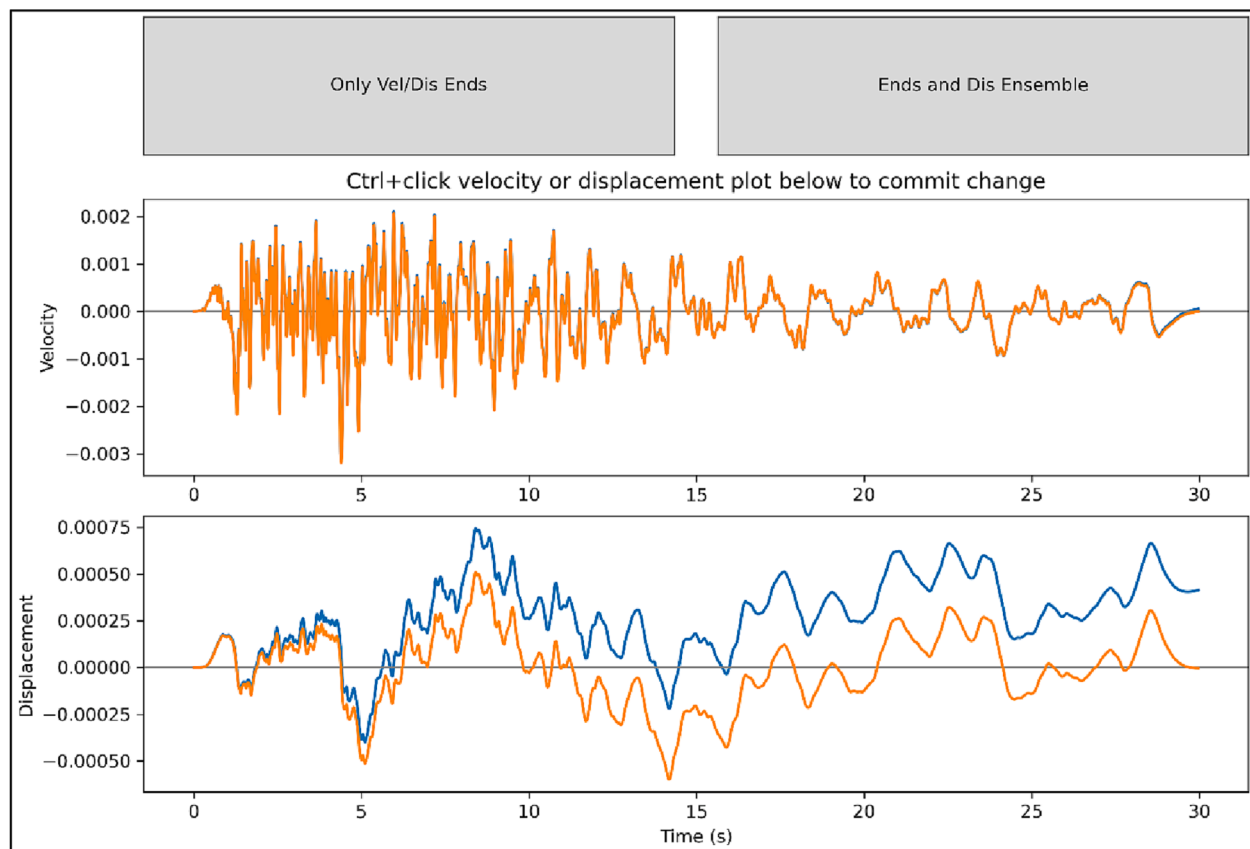


Fig. 14. Interface for baseline correction of the displacement time history using a Lagrange optimizer.

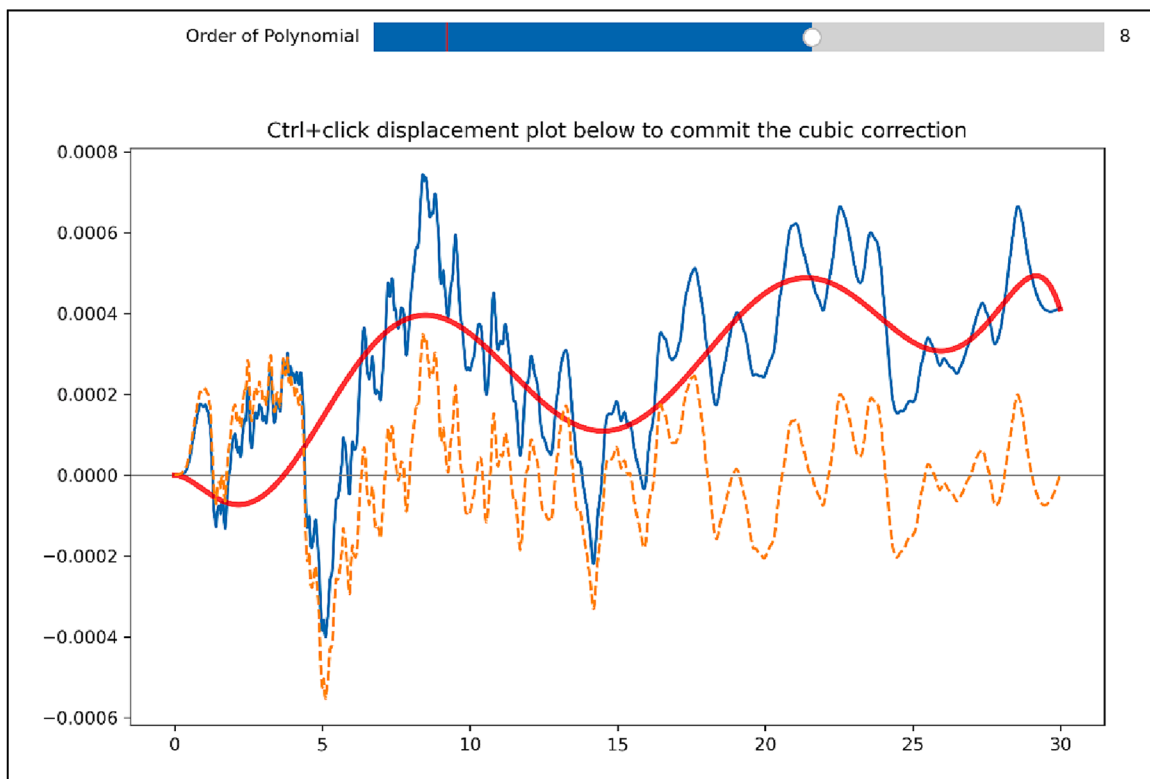


Fig. 15. Interface for detrending the displacement time history using polynomials.

back but then baseline correction would remove them again. To resolve this cyclic issue, GWM implemented a special method to add a wavelet at a selected frequency and at a selected time, which usually should be chosen in the middle of the acceleration time history. The amplitude of the wavelet can be interactively changed such that this wavelet would govern the RS comparison, and future iterations would then calculate a t_j around the selected time for this wavelet. This method does not have a specific physical basis, but it does help resolve the canceling effects of RS matching and baseline correction. Fig. 16 shows an example of this process to add an individual wavelet at selected frequency and selected time.

We have also implemented other tools in GWM, including adding Gaussian noises with standard deviations at 5% of instantaneous absolute values of the acceleration time history to enhance convergence, band-wise matching, applying split cosine envelop function, filtering high frequency content, stepping the RS matching process by one, five, or ten wavelets, adding a wavelet at a selected frequency but at a calculated time, performing the Option 1 Approach 2 RS check in NUREG-0800 Section 3.7.1, "Seismic Design Parameters" (USNRC, 2014b). Since these are not the main functions in GWM, they are not introduced in this paper. However, we would like to note that Python and its vast ecosystem for software development make the development of GWM easy. So as needs arise, GWM can be easily expanded for more capabilities.

6. Examples using RG 1.60 DRS

The shape of the RG 1.60 Horizontal DRS has several kinks that often present some challenges for the frequency domain RS matching algorithms to achieve close RS matches. The RG 1.60 DRS also shows a clear ZPA region after 33 Hz, and because the RG 1.60 DRS is specified as the 84-percentile RS, it is not admissible and the associated ZPA level is lower than what the frequency content in the amplifying region can achieve.

Fig. 17 shows that without ZPA flipping, GWM does not converge

with 1,200 wavelets and does not show any sign that a convergence would be achievable, as shown in Fig. 18 by the convergence history which stays flat after the first few wavelets. We also ran GWM up to 3,000 wavelets and did not achieve a convergence. The relative errors in the ZPA region become higher than those at other frequencies after some initial iterations, so GWM as a greedy approach selects that region to add additional wavelets to reduce the computed ZPA to the ZPA on the DRS. Because the RG 1.60 DRS is not admissible, it is unlikely to achieve a convergence in that region by adding wavelets. Therefore, ZPA flipping has to be turned on for GWM to focus on matching at other frequencies and achieve convergence.

With ZPA flipping, GWM used only 22 wavelets to achieve convergence when a [-10%, 30%] convergence range criterion was used, as shown by Fig. 19. This nonsymmetric convergence range is intended for design purposes. A tighter convergence range of [-5%, 15%], which is half of [-10%, 30%], made GWM to converge with 86 wavelets, nearly 4 times of that using the larger convergence range. Both cases required a minimum amount of execution time for GWM to converge.

With ZPA flipping and a 5% symmetric convergence criterion (i.e., a convergence range of [-5%, 5%]), GWM could only achieve convergence with 2,248 wavelets. When the convergence range changed from [-5%, 15%] to [-5%, 5%], the number of wavelets required for convergence increased significantly by 2,162. A 50% reduction of convergence criterion increased the effort by 22.5 times. Therefore, a convergence criterion as large as acceptable in practice should be used to achieve much faster convergence rate.

The kinks on the RG1.60 DRS pointing upwards create some minor challenges for the symmetric convergence criteria. In fact, had the convergence range [-5%, 5%] shifted upwards to [-2.5%, 7.5%], GWM would converge with 1,934 wavelets, 14% fewer than the symmetric convergence criterion.

7. Concluding remarks

We implemented GWM for fast and effective RS matching and used

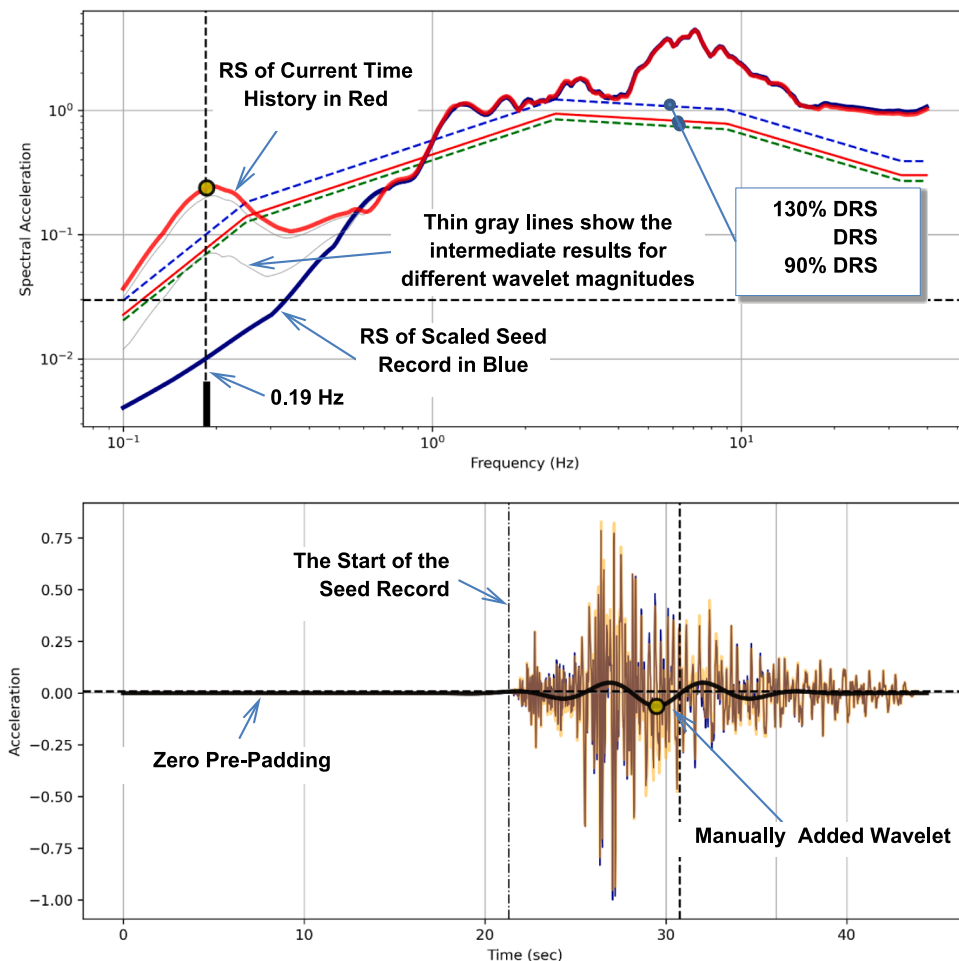


Fig. 16. Interactively adding a wavelet of 0.19 Hz with its center around 28 s. The magnitude of the wavelet can be changed by dragging the circle on the wavelet (shown in thick black curve) such that its RS is higher than the DRS as shown in the top plot.

GWM in a research that required RS matching of thousands of seed records. GWM utilizes the same wavelet formula as in the widely used RspMatch09 program, but takes some fundamentally different steps in the overall procedure. In contrast to RspMatch09 adding many wavelets in every iteration, GWM adds a single wavelet in each iteration that maximizes its effect on improving the RS comparison, and does not require solving an optimization problem as RspMatch09 and its predecessors do to determine the weights for the wavelets at all frequencies considered in the RS comparison.

More importantly, we identified ways to make GWM unconditionally robust, and achieved that by explicitly using the polarity and the time location of the oscillator peak response due to the wavelet. Due to stripping zero pre-padded portion of the resultant acceleration time history, numerically distorted high frequency wavelets, and ZPA flipping required for inadmissible DRS, the converged acceleration time histories may have drifts in the velocity and displacement time histories. These three issues may also impact other wavelet based methods. GMW implements various ways to make the baseline corrections as easy as a few mouse clicks. GWM is highly expandable as needs arise.

Benchmarked against the example provided with the RspMatch09 program, we found GWM to have major computational advantages over RspMatch09 even though GWM is implemented in the interpreted Python language while RspMatch09 was implemented in the compiled Fortran language. This example also shows that GWM uses a substantially smaller number of wavelets than RspMatch09 (46 versus 9,070, representing a 99.5% of saving) based on a 10% RS convergence threshold. For reference, RspMatch09 used 9,070 wavelets for the

example and achieved a maximum error of 13.1%, which is considered as a very low level of error for design purposes.

We applied GWM for other examples using the RG 1.60 horizontal DRS and demonstrated the need of ZPA flipping for inadmissible DRS. These examples also showed that the rate of convergence for RS matching is tremendously affected by the selection of RS convergence criteria. Therefore, a convergence criterion as large as acceptable in practice should be used to achieve fast convergence rate. The minimal RS matching criteria are a choice of the users and are often specified in codes and standards. For example, USNRC Standard Review Plan (2014b) describes the minimal RS matching criteria for seismic design time histories.

We emphasize that response spectrum matching is only one aspect in the development of acceptable acceleration time histories. There are other important aspects such as earthquake magnitude, source-to-site distance, site conditions, and in particular, checking the power spectral density functions. In general, because these aspects are well separated from the RS matching process, their assessment are usually performed outside of the RS matching methods. More details on these aspects can be found in Section 3.7.1., “Seismic Design Parameters,” Revision 4, of NUREG-0800, Standard Review Plan, U.S. Nuclear Regulatory Commission, Washington, D.C (USNRC, 2014b).

We had an exploratory trial of a different wavelet using an exponential taper function, and found it led to even smaller numbers of wavelets than the improved tapered cosine wavelet to achieve the same RS convergence criteria. A future effort will explore how different wavelets and their parametric variation can affect the convergence rate

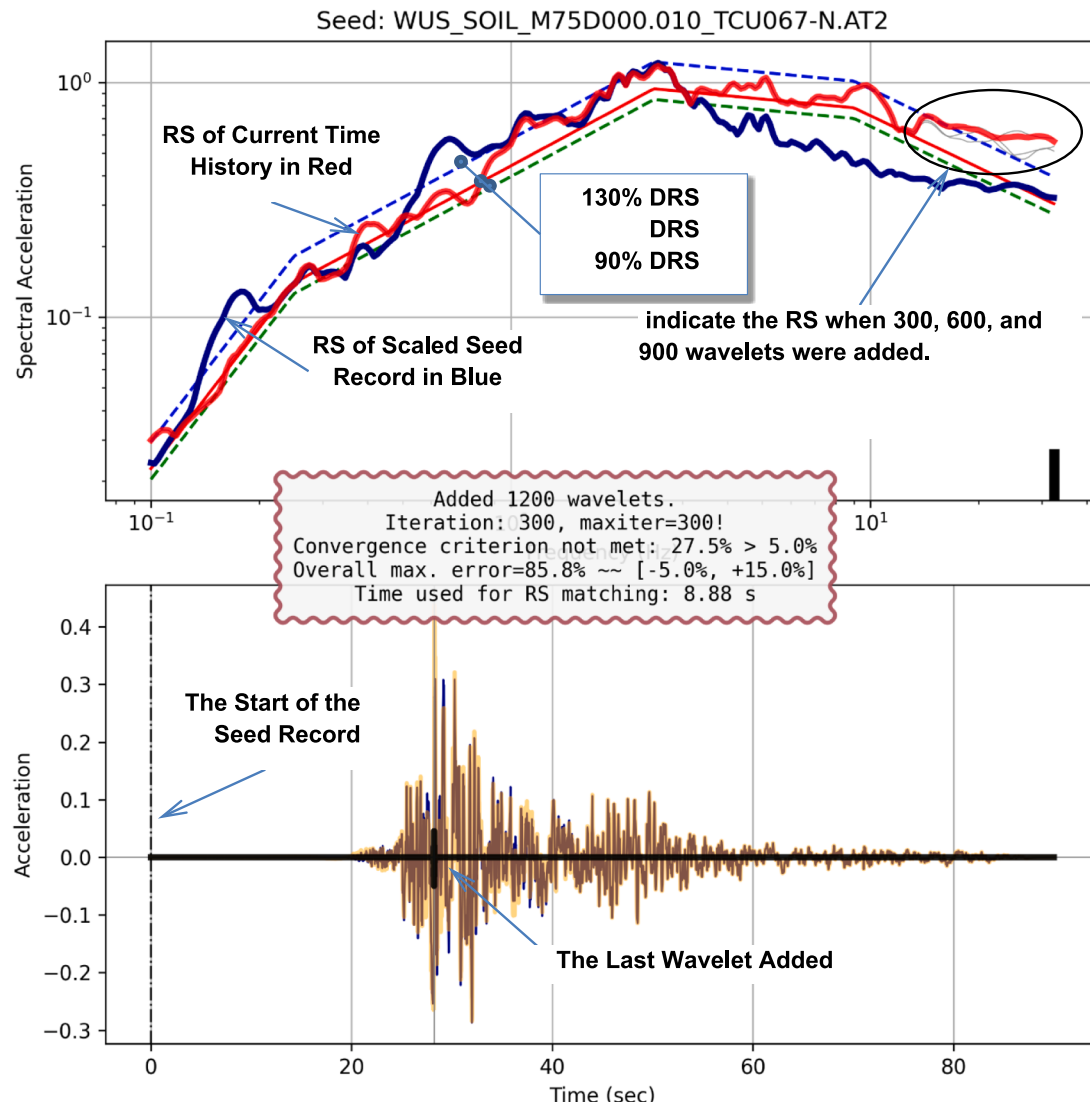


Fig. 17. Without ZPA flipping, GWM quickly stuck to adding wavelets at frequencies close to 33 Hz attempting to improve the unachievable RS match at the ZPA region. Because the relative error at the ZPA region is larger, GWM as a greedy approach does not try to improve RS matching at lower frequencies.

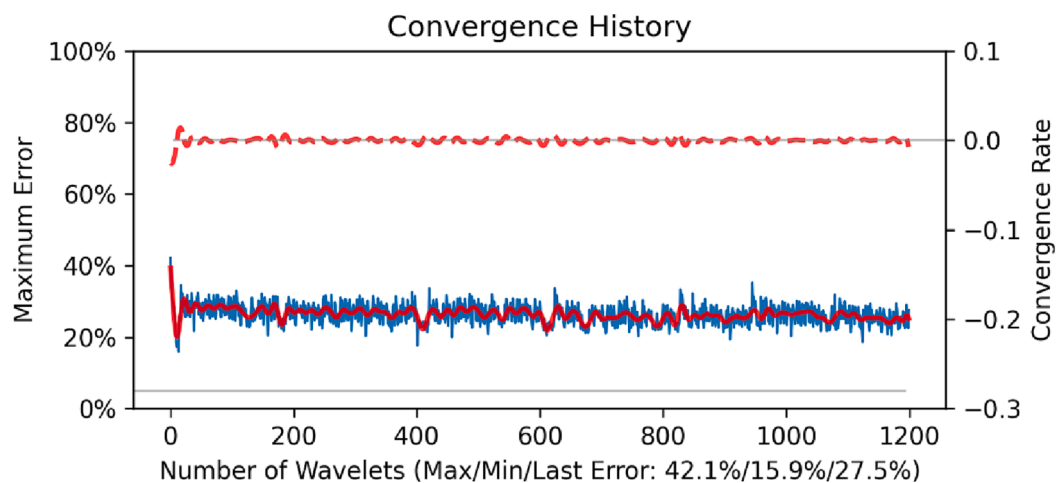


Fig. 18. Without ZPA flipping, the convergence history shows that GWM shows nearly no improvement after the initial quick reduction in the maximum error.

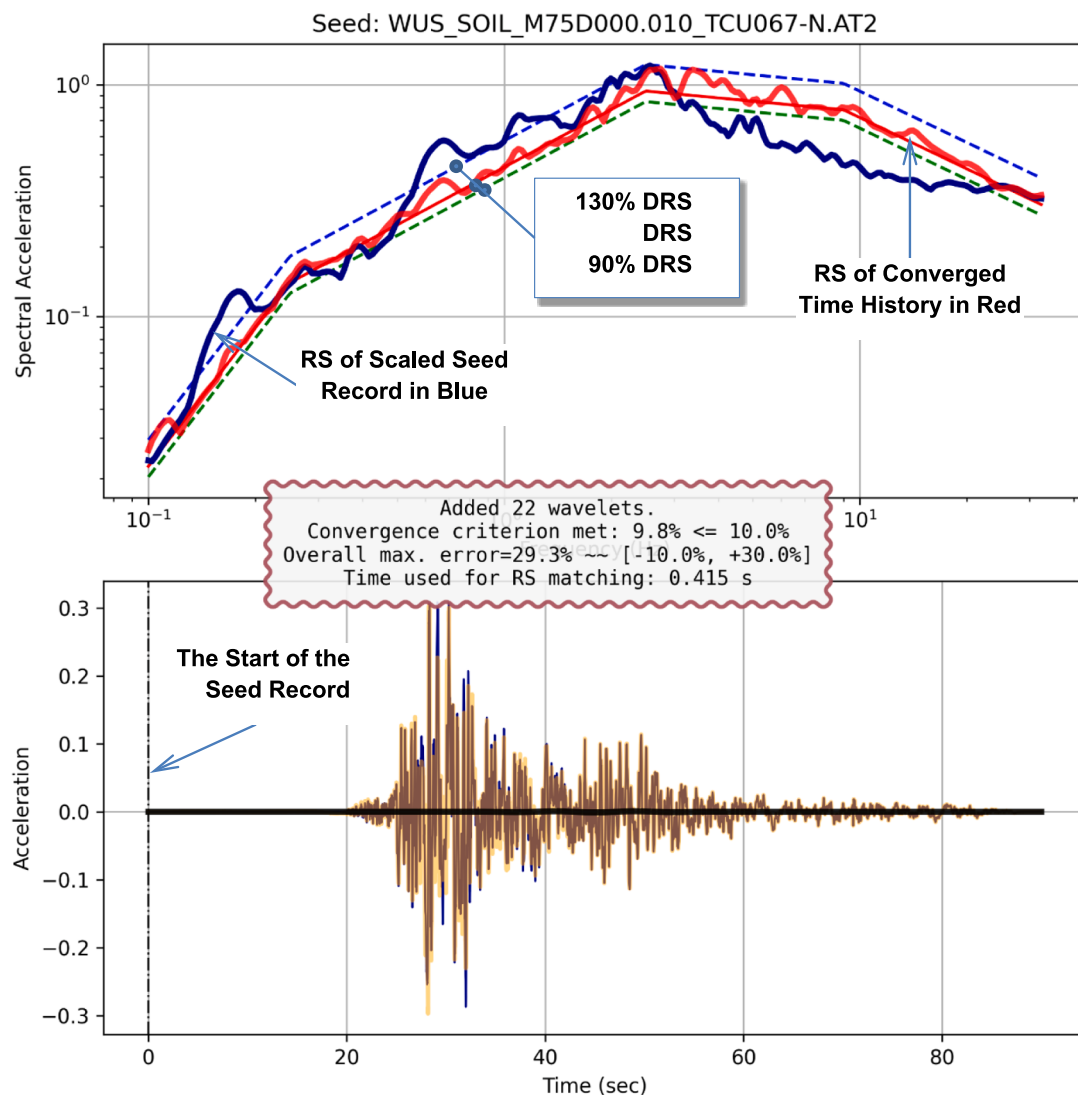


Fig. 19. With ZPA flipping and a [-10%, 30%] convergence range for design purposes, GWM used only 22 wavelets to achieve convergence.

of GWM.

Because GWM requires only a very small number of wavelets to achieve RS convergence and consequently introduces a minimal number of changes to the seed time histories, it makes possible a well separated treatment of power assurance and RS matching. The users of GWM can first introduce sufficient power to seed time histories based on the target PSD functions, and then apply GWM to achieve RS convergence criteria without much concern of making the final time histories deficient of power.

CRediT authorship contribution statement

Jinsuo Nie: Conceptualization, Methodology, Software, Investigation, Formal analysis, Validation, Visualization, Writing – original draft. **Vladimir Graizer:** Writing – review & editing. **Dogan Seber:** Writing – review & editing.

Declaration of Competing Interest

The authors declare that they have no known competing financial interests or personal relationships that could have appeared to influence the work reported in this paper.

Data availability

Code is not in a sharable form yet; however, we can consider to develop a sharable version if there is enough interest.

Acknowledgement

Dr. Jim Xu contributed significantly to our previous efforts that identified the research need for the automated response spectrum matching method described in this paper. His support was tremendous and is greatly appreciated. The authors thank the editor and two anonymous reviewers for their suggestions and critical comments helping to improve the article.

Disclaimer

The findings and opinions expressed in this paper are those of the authors, and do not necessarily reflect the view of the U.S. Nuclear Regulatory Commission.

References

- Abrahamson, N.A., 1992. Non-stationary spectral matching. *Seismol. Res. Lett.* 63 (1), 30.
- Al Atik, L., Abrahamson, N.A., 2010. An improved method for nonstationary spectral matching. *Earthq. Spectra* 26 (3), 601–617.
- ASCE/SEI 41-06 , 2007. Seismic Rehabilitation of Existing Buildings. American Society of Civil Engineers, Reston, VA.
- ASCE/SEI 43-19 , 2019 . Seismic Design Criteria for Structures, Systems, and Components in Nuclear Facilities . American Society of Civil Engineers , Reston, VA .
- ASCE/SEI 4-16 , 2017 . Seismic Analysis of Safety-Related Nuclear Structures . American Society of Civil Engineers , Reston, VA .
- ASCE/SEI 7-05 , 2006, Minimum Design Loads for Buildings and Other Structures. American Society of Civil Engineers, Reston, VA.
- Borsoi, L., Ricard, A. (1985). "A simple accelerogram correction methods to prevent unrealistic displacement shift", the 8th Structural Mechanics in Reactor Technology, SMiRT8, Vol.K(a), Paper K2/7, Brussels.
- Hancock, J., Watson-Lamprey, J., Abrahamson, N.A., Bommer, J.J., Markatis, A., McCoy, E., Mendis, R., 2006. An improved method of matching response spectra of recorded earthquake ground motion using wavelets. *J. Earthq. Eng.* 10 (s1), 67–89.
- Huang, N.E., Shen, Z., Long, S.R., Wu, M.C., Shih, H.H., Zheng, Q., Yen, N.-C., Tung, C.C., Liu, H.H., 1998. The empirical mode decomposition and the Hilbert spectrum for nonlinear and non-stationary time series analysis. *Proc. Math. Phys. Eng. Sci.* 454 (1971), 903–995.
- Kaul, M.K., 1978. Spectrum-consistent time-history generation. *J. Eng. Mech. Div.* 104 (4), 781–788.
- Li, B., Xie, W.-C., Pandey, M.D., 2016. Generate tri-directional spectra-compatible time histories using HHT method. *Nucl. Eng. Des.* 241, 73–85.
- Li, B., Ly, B.-L., Xie, W.-C., Pandey, M.D., 2017. Generating spectrum-compatible time histories using eigenfunctions. *Bull. Seismol. Soc. Am.* 107 (3), 1512–1525.
- Lilhanand, K., Tseng, W.S. (1988). Development and application of realistic earthquake time histories compatible with multiple-damping design spectra, *Proc. of the Ninth World Conf. on Earthquake Engineering, Tokyo, Japan*, 2–9 August 1988.
- NEHRP Consultants Joint Venture (2011). Selecting and Scaling Earthquake Ground Motions for Performing Response-History Analyses. *National Institute of Standards and Technology, NIST GCR 11-917-15*, 256 p.
- Ni, S.H., Xie, W.C., Pandey, M.D., 2013. Generation of spectrum compatible earthquake ground motions considering intrinsic spectral variability using Hilbert-Huang transform. *Struct. Saf.* 42, 45–53.
- Nie, J., Pires, J., Seber, D. (2019). "Understanding the assumptions in input response spectra for seismic time history analyses." the 25th Structural Mechanics in Reactor Technology, SMiRT25, Charlotte, NC, August 4-9, 2019.
- Nie, J., Xu, J., Graizer, V., Seber, D. (2020). "Estimating stable mean responses for linear structural systems by using limited number of acceleration time histories." 2020 ASME Pressure Vessels and Piping Division Conference, PVP2020, Virtual Meeting.
- Nie, J., Xu, J., Graizer, V., Seber, D. (2023). "Uncertainties in In-structure Response Spectra Due to Uncertainties in Input Motion Amplitude and Phase Spectra." 2023 ASME Pressure Vessels and Piping Division Conference, PVP2023, Atlanta, Georgia, July 16–21, 2023 (in press).
- Nie, J. (2020) "Assessment of Artificial Acceleration Time History Guidance in Standard Review Plan Section 3.7.1, "Seismic Design Parameters," *RIL 2019-01*, Rev. 1, August 2020.
- Pozzi, M., Der Kiureghian, A. (2013). "Response spectrum compatible PSD for high-frequency range," *Transactions, SMiRT-22*, San Francisco, California.
- Shahbazian, A., Pezeshk, S., 2010. Improved velocity and displacement time histories in frequency domain spectral-matching procedures. *Bull. Seismol. Soc. Am.* 100 (6), 3213–3223.
- Suarez, L.E., Montejano, L.A., 2005. Generation of artificial earthquakes via the wavelet transform. *Int. J. Solids Struct.* 42 (21–22), 5905–5919.
- U.S. Nuclear Regulatory Commission (USNRC) (1989). Recommendations for Resolution of Public Comments on USI A-40, "Seismic Design Criteria," *NUREG/CR-5347*, U.S. Nuclear Regulatory Commission, Washington, D.C.
- USNRC (2014a). Design Response Spectra for Seismic Design of Nuclear Power Plants. *RG 1.60 (rev. 2)*, U.S. Nuclear Regulatory Commission, Washington, D.C.
- USNRC (2014b). Section 3.7.1., "Seismic Design Parameters," Revision 4, of *NUREG-0800*, Standard Review Plan, U.S. Nuclear Regulatory Commission, Washington, D.C.
- Vemuri J., and Kolluru S. (2020). Evaluation of Ground Motion Scaling Techniques. In: A. Prashant et al. (eds.), *Advances in Computer Methods and Geomechanics*, Lecture Notes in Civil Engineering 55, 525–535.
- Wu, Z., Huang, N.E., 2008. Ensemble empirical mode decomposition: a noise-assisted data analysis method. *Adv. Adaptive Data Analysis* 1 (1), 1–41.